



Scottish Universities Environmental Research Centre

**OSL characterisation of two fluvial
sequences of the River Usumacinta
in its middle catchment (SE Mexico)**

Luminescence Laboratory Report

January 2014

**T.C. Kinnaird¹, E. Muñoz-Salinas², D.C.W. Sanderson¹,
Castillo Rodriguez, M.² and Cruz-Zaragoza, E.³**

¹SUERC, East Kilbride, G75 0QF

²Instituto de Geología, Universidad Nacional Autónoma de México,

³Instituto de Ciencias Nucleares, Universidad Nacional Autónoma de México

East Kilbride Glasgow G75 0QF Telephone: 01355 223332 Fax: 01355 229898



The University of Glasgow, charity number SC004401



The University of Edinburgh is a charitable body,
registered in Scotland, with registration number SC005336

Preface. This is the second in a series of two reports which describe the luminescence methodologies used to construct chronologies for sediment stratigraphies in the terrace deposits of the Usumacinta and Grijalva Rivers (SE Mexico). The background to the investigation is provided in the previous report:

Kinnaird, T.C., Muñoz-Salinas, E. and Sanderson, D.C.W. 2012. Using optically stimulated luminescence to unravel sedimentary processes of the Usumacinta and Grijalva Rivers (SE Mexico). SUERC dating report, SUERC, p. 1-29.

Summary

The report summarizes luminescence profiling, initially using a SUERC PPSL system in Mexico, and laboratory analysis at SUERC, used to characterise the stratigraphy and interpret sedimentary processes in terrace deposits of the Usumacinta River, SE Mexico. This was then followed, by quantitative quartz OSL SAR dating of five sediment samples, aimed at defining the chronological framework of two sedimentary sequences, USU13-1 and USU13-2. In the wider region, the middle catchment of the Usumacinta River, contains numerous archaeological sites dating to the Maya Classic Period, including Bonampak, Yaxchilan and Piedras Negras. The broader aim of the investigation is to assess whether the two fluvial sequences contain a proxy record of environmental change through the archaeological period of interest.

Initial luminescence profiling revealed that the stratigraphy in each profile was complex, reflecting multiple cycles of deposition, with signal maxima, followed by tails to lower intensities, possibly indicating deposition during extreme flood events, interleaved with periods of slower sedimentation, and potentially better luminescence resetting. Laboratory profiling reproduced the apparent maxima/trends in the field profiling dataset, confirming that both sections record complex depositional histories. Furthermore, the variations in stored dose estimates, and luminescence sensitivities with depth, confirm that the sections do not record simple age-depth progressions. Quantitative quartz OSL SAR dating was undertaken on five sediment samples. Given the information obtained from the field- and laboratory-profiles it is not surprising that the equivalent dose distributions for each sample showed considerable scatter, particularly so for the second section, USU13-2. Nevertheless, through statistical analysis, individual quartz OSL SAR ages were obtained for each sample. Individual dates fall into the Mayan Post-Classical Period to early modern Period, with statistical combinations pointing to a late 15th century accumulation of USU13-1, and the 18th century accumulation of the sediment within USU13-2. Interestingly, the three samples from section USU13-2, all show some aliquots which tail to higher equivalent doses; furthermore, in each sample, the mean value determined for this component is similar, suggesting that the sediment sampled in USU13-2, may be sourced from a 15th century or older accumulation upstream.

Contents

1.	Introduction.....	2
2.	Sampling	2
3.	Calibrated laboratory luminescence screening measurements	4
3.1.	Methodology	4
3.2.	Results.....	4
4.	Quartz SAR measurements	8
4.1.	Sample preparation	8
4.1.1.	Water contents	8
4.1.2.	HRGS and TSBC Sample Preparation.....	8
4.1.3.	SAR Sample Preparation	8
4.2.	Measurements and determinations.....	8
4.2.1.	Dose rate determinations.....	8
4.2.2.	SAR luminescence measurements	9
4.3.	Results.....	11
4.3.1.	Dose rates	11
4.3.2.	Single aliquot equivalent dose determinations	12
4.3.3.	Age determinations	13
5.	Discussions and conclusions.....	15
6.	References.....	14
	Appendix A: Laboratory Profiling Results	18
A.1	SUTL2582/SUTL2586 Quartz.....	18
A.2	SUTL2582/SUTL2586 Polymineral	19
	Appendix B: Dose Response Curves	20
B.1	SUTL2580.....	20
B.2	SUTL2581	20
B.3	SUTL2583	21
B.4	SUTL2584.....	21
B.5	SUTL2585	22
	Appendix D: Radial plots.....	23
D.1	Radial plot for SUTL2580	23
D.2	Radial plot for SUTL2581	23
D.3	Radial plot for SUTL2583	24
D.4	Radial plot for SUTL2584	24
D.5	Radial plot for SUTL2585	25

List of Figures

Figure 1-1: Location of profiles USU13-1 and USU13-2 in the Usumacinta Middle River Basin (Southern Mexico)	2
Figure 2-1: Section USU13-1, showing the distribution of the full dating and laboratory profiling samples	2
Figure 2-2: Section USU13-2, showing the distribution of the full dating and laboratory profiling samples	3
Figure 2-3: Net IRSL signal intensities obtained for profiling samples taken at ~10 cm spacing through profiles USU13-1 and USU13-2	3
Figure 3-1: Laboratory profiling results, Usumacinta River (Section USU13-1).....	6
Figure 3-2: Laboratory profiling results, Usumacinta River (Section USU13-2)	7

List of Tables

Table 2-1: SUTL sample reference numbers	3
Table 4-1: Quartz Single Aliquot Regenerative (SAR) Sequence (Discs 1 -16).....	10
Table 4-2: Activity and equivalent concentrations of K, U and Th determined by HRGS.....	11
Table 4-3: Infinite matrix dose rates determined by HRGS and TSBC.	12
Table 4-4: Water contents, and effective beta and gamma dose rates following water correction.	12
Table 4-5: SAR quality parameters. Standard errors given.	13
Table 4-6: OSL age determinations for samples SUTL2508-09 and 2511-13	14

1. Introduction

This report is concerned with optically stimulated luminescence (OSL) investigations of sediment collected from terrace deposits of the Usumacinta river, in its middle catchment (SE Mexico; Fig. 1-1). Numerous archaeological sites, dating to the Mayan Classical Period, are located in the Middle Usumacinta Basin, including the centres of Bonampak, Yaxchilan and Piedras Negras. The objective of the luminescence investigations is to define a relative chronology for sediments represented in two fluvial sections, USU13-1 and USU13-2. The two sections are located at strategic positions relative to the Mayan archaeological centres: USU13-1, is located at the confluence of the Salinas and Usumacinta rivers; USU13-2, is located 90 km downstream of USU13-1, 12 km from Yaxchilan, 22km from Bonampak and 56 km from Piedras Negras.

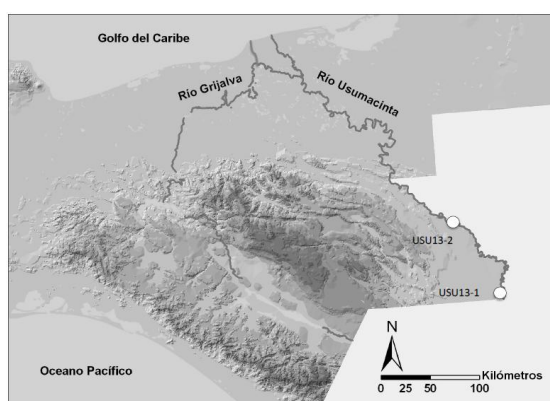


Figure 1-1: Location of profiles USU13-1 and USU13-2 in the Usumacinta Middle River Basin (Southern Mexico)

The broader aim of the investigation is to assess whether the two fluvial sequences contain a proxy record of environmental change through the archaeological periods of interest.

2. Sampling

Sampling was undertaken by Esperanza Muñoz-Salinas during the early summer of 2013. Photographs of the two sediment stratigraphies are reproduced in figures 2-1 and 2-2. Samples were submitted to the luminescence laboratories at the Scottish Universities Environmental Research Centre (SUERC) for dating in July 2013. Sample numbers, contexts, and unique laboratory code (assigned on receipt) are listed in Table 2-1.



Figure 2-1: Section USU13-1, showing the distribution of the full dating and laboratory profiling samples

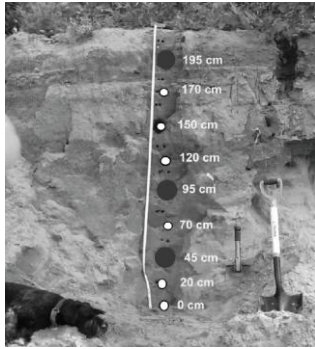


Figure 2-2: Section USU13-2, showing the distribution of the full dating and laboratory profiling samples

Depth relative to datum	Laboratory profiling sample no. / laboratory code	Laboratory dating sample / laboratory code	Height relative to datum	Laboratory profiling sample no. / laboratory code	Laboratory dating sample / laboratory code
<i>Usumacinta section, USU13-1</i>			<i>Usumacinta section, USU13-2</i>		
0.20*	SUTL2582A		1.95		SUTL2583
0.45*		SUTL2580	1.70	SUTL2586A	
0.60*	SUTL2582B		1.50	SUTL2586B	
0.80*	SUTL2582C		1.20	SUTL2586C	
1.10*		SUTL2581	0.95		SUTL2584
1.40*	SUTL2582D		0.70	SUTL2586D	
			0.45		SUTL2585
			0.20	SUTL2586E	
			0	SUTL2586F	

Table 2-1: SUTL sample reference numbers

Following fieldwork, Esperanza Muñoz-Salinas made use of the SUERC PPSL system at the Research Institute of Nuclear Sciences (National Autonomous University of Mexico), to explore IRSL net signal variations within each fluvial sequence, in a similar manner to that described by Sanderson and Murphy (2010) using the SUERC portable OSL reader, to characterise the stratigraphy in each, and identify sedimentary phases and potential horizons for dating (Fig. 2-3).

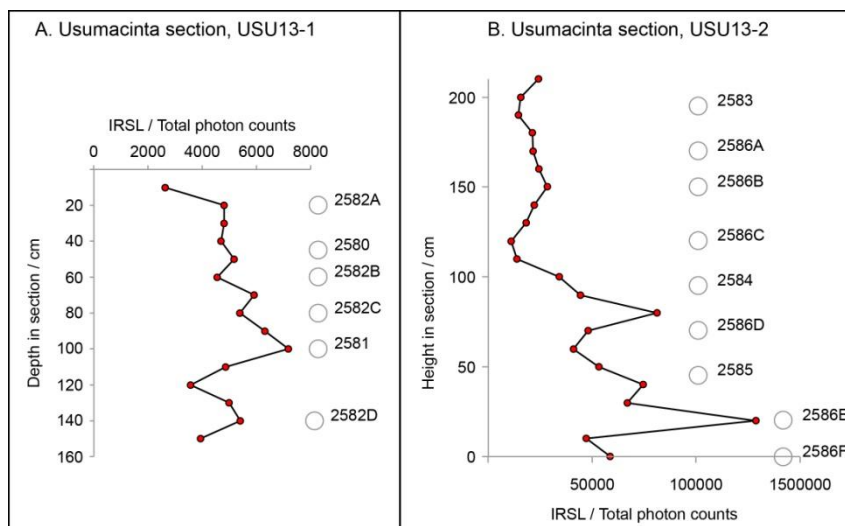


Figure 2-3: Net IRSL signal intensities obtained for profiling samples taken at ~10 cm spacing through profiles USU13-1 and USU13-2

In both profile, there is a large spread in net signal intensities with depth, reflecting variable zeroing of the sediment on deposition, and/or sensitivity variations, controlled by grain size fluctuations. The first profile, USU13-1, shows only a slight increase in IRSL net luminescence signals with depth, with a notable maxima in net signals through the interval 20-120 cm depth. It will be important to establish whether these variations in net IRSL signals correspond to similar variations in luminescence sensitivities and stored dose estimates. Interestingly, the second profile USU13-2, shows a broad increase in luminescence signals with depth, implying that overall, there may be a broad increase with age with depth.

The positions of the profiling and full dating samples are shown, relative to the field profiling dataset, for sections USU13-1 and USU13-2, in figure 2-3. In both profiles the positions of the profiling and dating samples encompass a range in IRSL net signals.

3. Calibrated laboratory luminescence screening measurements

3.1. Methodology

All sample handling and preparation was conducted under safelight conditions in the SUERC luminescence dating laboratories. The profiling samples were wet sieved to extract the 90-250 μm fractions, which were then treated with 1M HCl for 10 minutes. The samples were split into two fractions, one for polymineral analysis and one for quartz analysis. The quartz subsample was treated with 40% HF for 40 minutes, to dissolve the less chemically resistant minerals and to etch the outer part of the grains. The HF etched material was then treated with 1 M HCl for 10 minutes to dissolve any precipitated fluorides. The grains were presented for measurement on 10 mm in diameter stainless steel discs.

Luminescence sensitivities (Photon Counts per Gy) and stored doses (Gy) were evaluated from paired aliquots of the HF-etched quartz and polymineral fractions, using Risø DA-15 automatic readers. The readout cycles comprised a natural readout, followed by readout cycles for a nominal 1Gy test dose, a 5Gy regenerative dose, and a further 1Gy test dose. For the quartz samples, a 240°C preheat was used with 60s OSL measurements using the blue LEDs. For the polymineral samples, a 260°C preheat was followed by 60s OSL measurements using the IR LEDs at 50°C, the IR LEDs at 225°C (the post-IR IRSL signal), the blue LEDs at 125°C, and a TL measurement to 500°C.

3.2. Results

The data are presented graphically in figures 4-1 and 4-2, for the two profiles respectively. The data is tabulated in Appendix A.

The apparent trends and maxima observed in the field profiling dataset for the upper part of profile USU13-1 are reproduced in the laboratory profiling dataset, reflecting the sections complex stratigraphy. Notably, the lowest quartz stored dose estimates obtained from within this section, were derived from sediment sampled at a depth of 60 cm; this raises several questions: (i) do the stored dose values obtained from height within the sequence represent accumulations that were poorly reset on deposition, and

that the stored dose values obtained at a depth of 60 cm, represent the maximum age of the succession? or, (ii) are the variations in stored dose estimates controlled by variations in the environmental dose rate, such that the units are similar in age? In support of the former, the quartz OSL:TL ratio, which potentially encodes information on the bleachability of the quartz luminescence signals, is lowest for the horizon at 60cm, suggesting that this horizon is better bleached. Full dose rate determinations will be made at each of the full dating sample positions, and provide a means to test these two hypotheses. Intriguingly, the IRSL stored dose estimates from the same horizon, are larger than those obtained at height in the succession, reproducing the trends observed in the field IRSL profiling dataset. The data imply that there is an inverse correlation between minima in quartz OSL stored dose values, and maxima in polymineral IRSL stored dose values; implying that caution must be taken in interpreting variations within net IRSL signal intensities in the field profiling dataset in terms of trends within the quartz system.

The trends within the field and laboratory profiling datasets deviate in the lower part of the profile: the field profiling dataset only records a slight increase in net luminescence signals between the top and bottom of the profile; whereas, there is a notable increase in quartz stored dose values between the well-bleached horizon at 60 cm, and the lowermost sampled horizon. A note of caution, the field profiling dataset extends the profile beneath that sampled for laboratory profiling; if the radioactivity of the material sampled through the section is similar, and similar environmental dose rates were received at each of the sampling locations, then this may imply that the laboratory profiling samples, and the full dating samples, do not encompass the full range of net IRSL signal variations, and may slightly overestimate the age of the succession.

The broad progression in luminescence signals with depth through the second profile, USU13-2, was taken as evidence that the stratigraphy in the second profile was slightly less complex. However, the apparent trends and maxima in the calibrated luminescence dataset, indicate that the stratigraphy within the second profile is as complex as that recorded in profile USU13-1. Minima in quartz OSL stored dose values were obtained from strata at 75 cm depth in the section (SUTL2586/C); and maxima in quartz OSL stored dose estimates were obtained from strata at 125 cm depth in the section (SUTL2586/D), indicating that this sediment experienced variable resetting at deposition. If the radioactivity of the material sampled is consistent through the profile, then the variations in quartz OSL stored dose values will be driven largely by different bleaching conditions at deposition. As in USU13-1, there would appear to be an inverse correlation between quartz OSL stored dose values, and polymineral IRSL stored dose values.

A comment on the position of the full dating samples in relation to the laboratory profiling samples: given the complexity of the sampled stratigraphy, it would be unwise to assume that the quartz OSL ages will show a normal age-depth progression. For example, SUTL2584 is located on the leading edge of an age-depth progression above a maxima in the field and laboratory profiling datasets (SUTL2584, 100 cm depth - 2586/E, 175 cm depth), and one may expect this to return a luminescence age out of chronological sequence.

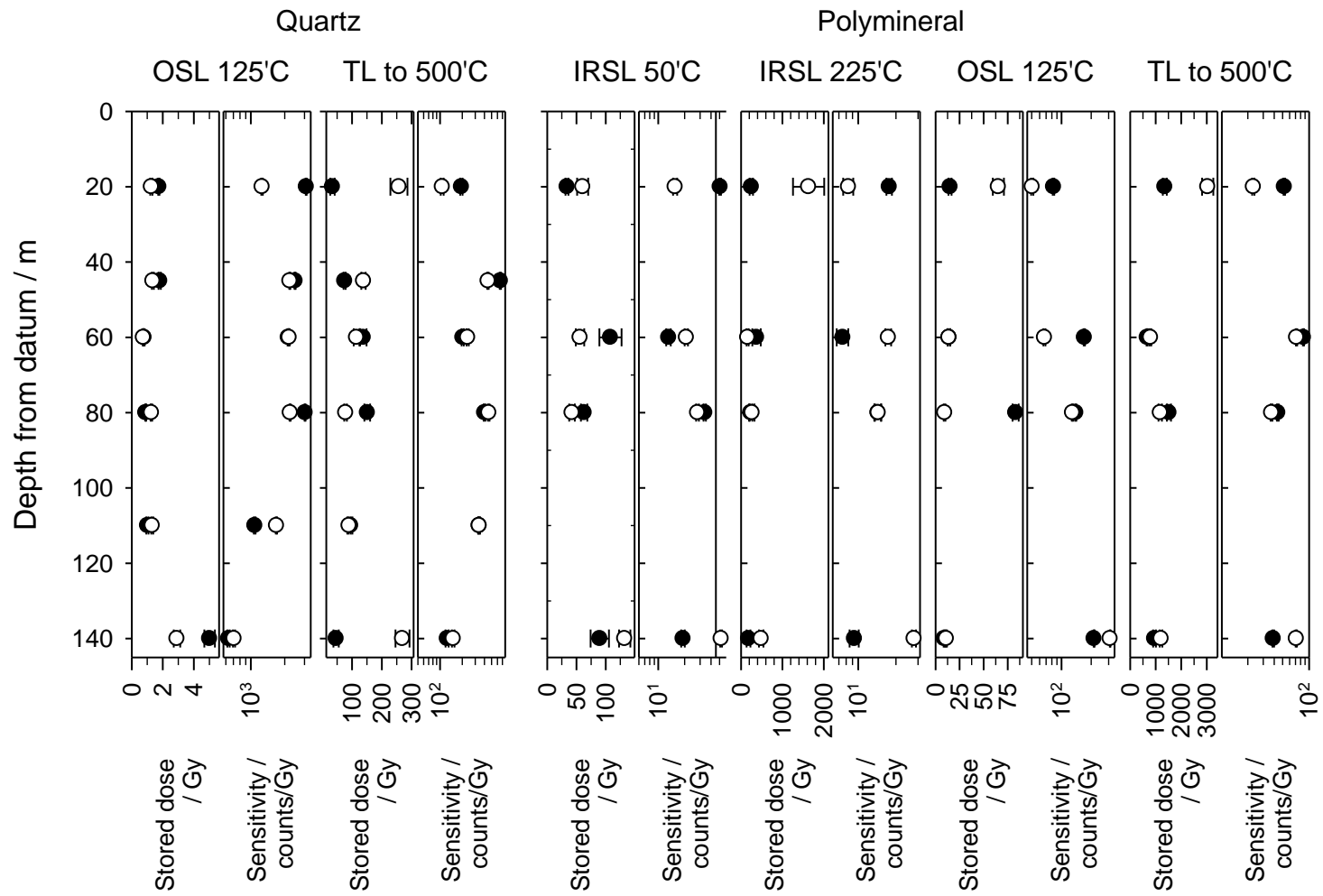


Figure 3-1: Laboratory profiling results, Usumacinta River (Section USU13-1).

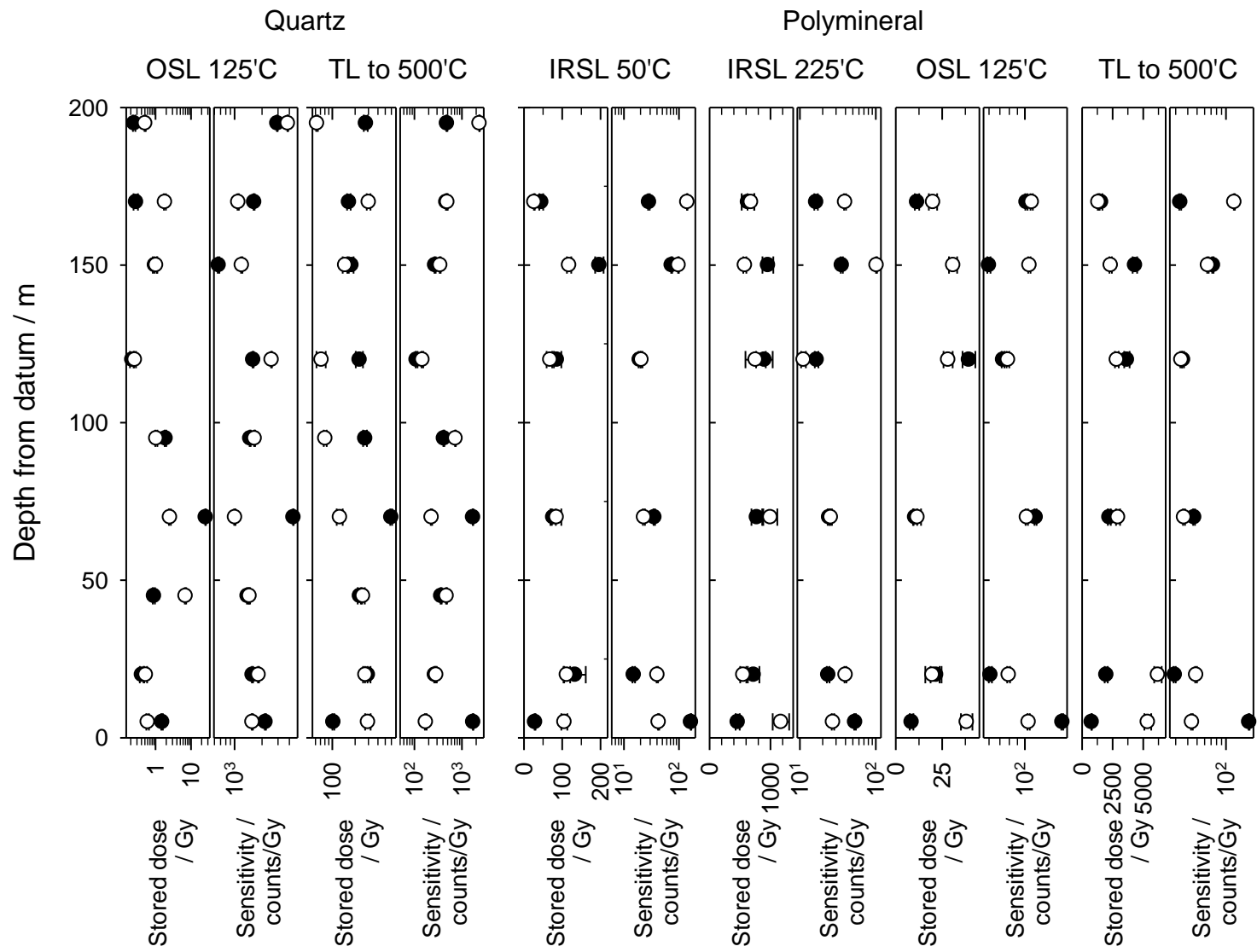


Figure 3-2: Laboratory profiling results, Usumacinta River (Section USU13-2)

4. Quartz SAR measurements

4.1. Sample preparation

All sample handling and preparation was conducted under safelight conditions in the SUERC luminescence dating laboratories.

4.1.1. Water contents

Bulk samples were weighed, saturated with water and re-weighed. Following oven drying at 50 °C to constant weight, the actual and saturated water contents were determined as fractions of dry weight. These data were used, together with information on field conditions to determine water contents and an associated water content uncertainty for use in dose rate determination.

4.1.2. HRGS and TSBC Sample Preparation

Bulk quantities of material, weighing c. 100-125 g, were removed from each full dating sample for environmental dose rate determinations. This material was placed in an oven to dry to constant weight. Approximately 100 g of dried material from each sample was weighed into a HDPE pot for a high-resolution gamma spectrometry (HRGS) measurement. From each of these samples, 20 g of material was temporarily removed and used in thick source beta counting (TSBC; Sanderson, 1988). This material was then returned to the relevant pot, sealed with epoxy resin and left for 3 weeks prior to measurement to allow equilibration of ²²²Rn daughters.

4.1.3. SAR Sample Preparation

Approximately 20g of material was removed for each tube and processed for luminescence measurements, to separate sand-sized quartz and feldspar grains. The sample was wet sieved to obtain the 90-150 and 150-250 µm fractions. The 150-250 µm sub-sample was treated with 1 M hydrochloric acid (HCl) for 10 minutes, 15% hydrofluoric acid (HF) for 15 minutes, and 1 M HCl for a further 10 minutes. This etched material was then centrifuged in sodium polytungstate solutions of ~2.51, 2.58, 2.62, and 2.74 gcm⁻³, to obtain concentrates of potassium-rich feldspars (2.51-2.58 gcm⁻³), sodium feldspars (2.58-2.62 gcm⁻³) and quartz plus plagioclase (2.62-2.74 gcm⁻³). The selected quartz fraction was then subjected to further HF and HCl washes (40% HF for 40mins, followed by 1M HCl for 10 mins). All materials were dried at 50°C and transferred to Eppendorf tubes. 16 aliquots were produced for each sample.

4.2. Measurements and determinations

4.2.1. Dose rate determinations

Dose rates were measured in the laboratory using HRGS and TSBC. Full sets of laboratory dose rate determinations were made for samples SUTL2580-81 and SUTL2583-85.

HRGS measurements were performed using a 50% relative efficiency “n” type hyper-pure Ge detector (EG&G Ortec Gamma-X) operated in a low background lead shield with a copper liner. Gamma ray spectra were recorded over the 30 keV to 3 MeV range from each sample, interleaved with background measurements and measurements from SUERC Shap Granite standard in the same geometries. Counting times of 80ks per sample were used. The spectra were analysed to determine count rates from the major line emissions from ^{40}K (1461 keV), and from selected nuclides in the U decay series (^{234}Th , ^{226}Ra + ^{235}U , ^{214}Pb , ^{214}Bi and ^{210}Pb) and the Th decay series (^{228}Ac , ^{212}Pb , ^{208}Tl) and their statistical counting uncertainties. Net rates and activity concentrations for each of these nuclides were determined relative to Shap Granite by weighted combination of the individual lines for each nuclide. The internal consistency of nuclide specific estimates for U and Th decay series nuclides was assessed relative to measurement precision, and weighted combinations used to estimate mean activity concentrations (Bq kg^{-1}) and elemental concentrations (% K and ppm U, Th) for the parent activity. These data were used to determine infinite matrix dose rates for alpha, beta and gamma radiation.

Beta dose rates were also measured directly using the SUERC TSBC system (Sanderson, 1988). Sample count rates were determined with six replicate 600 s counts for each sample, bracketed by background measurements and sensitivity determinations using the Shap Granite secondary reference material. Infinite-matrix dose rates were calculated by scaling the net count rates of samples and reference material to the working beta dose rate of the Shap Granite ($6.25 \pm 0.03 \text{ mGy a}^{-1}$). The estimated errors combine counting statistics, observed variance and the uncertainty on the reference value.

The dose rate measurements were used in combination with the assumed burial water contents, to determine the overall effective dose rates for age estimation. Cosmic dose rates were evaluated by combining latitude and altitude specific dose rates ($0.181 \pm 0.01 \text{ mGy a}^{-1}$) for the site with corrections for estimated depth of overburden using the method of Prescott and Hutton (1994).

4.2.2. SAR luminescence measurements

All measurements were conducted using a Risø DA-15 automatic reader equipped with a $^{90}\text{Sr}/^{90}\text{Y}$ β -source for irradiation, blue LEDs emitting around 470 nm and infrared (laser) diodes emitting around 830 nm for optical stimulation, and a U340 detection filter pack to detect in the region 270-380 nm, while cutting out stimulating light (Bøtter-Jensen et al., 2000). For each sample, equivalent dose determinations were made on sets of 16 aliquots per sample, using a single aliquot regeneration (SAR) sequence (cf Murray and Wintle, 2000). According to this procedure, the OSL signal level from an individual disc is calibrated to provide an absorbed dose estimate (the equivalent dose) using an interpolated dose-response curve, constructed by regenerating OSL signals by beta irradiation in the laboratory. Sensitivity changes which may occur as a result of readout, irradiation and preheating (to remove unstable radiation-induced signals) are monitored using small test doses after each regenerative dose. Each measurement is standardised to the test dose response determined immediately after its readout, to compensate for observed changes in sensitivity during the laboratory measurement sequence. For the purposes

of interpolation, the regenerative doses are chosen to encompass the likely value of the equivalent (natural) dose (determined in the initial laboratory characterisation study, see section 4). A repeat dose point is included to check the ability of the SAR procedure to correct for laboratory-induced sensitivity changes (the ‘recycling test’; table 5-1), a zero dose point is included late in the sequence to check for thermally induced charge transfer during the irradiation and preheating cycle (the ‘zero cycle’; table 5-1), and an IR response check is included to assess the magnitude of non-quartz signals. Regenerative dose response curves were constructed using doses of 1, 5, 10 and 30 Gy, with a test dose of 2 Gy (Table 5-1).

Aliquot	Operation	Cycle: Details	1	2	3	4	5	6	7	8
			Natural					Zero	Recycling	IR Response
1-20	Regenerative Dose	"X" Gy ⁹⁰ Sr/ ⁹⁰ Y	no	1	5	10	30	0	5	5
1-5	Preheat	200°C for 30s	yes	yes	yes	yes	yes	yes	yes	yes
6-10	Preheat	220°C for 30s	yes	yes	yes	yes	yes	yes	yes	yes
11-15	Preheat	240°C for 30s	yes	yes	yes	yes	yes	yes	yes	yes
16-20	Preheat	260°C for 30s	yes	yes	yes	yes	yes	yes	yes	yes
1-20	Measurement	OSL 60s at 125°C	yes	yes	yes	yes	yes	yes	yes	yes
1-20	Measurement	IRSL 60s at 50°C	no	no	no	no	no	no	no	yes
1-20	Test Dose (Td)	"X" Gy ⁹⁰ Sr/ ⁹⁰ Y	2	2	2	2	2	2	2	2
1-5	Td Preheat	200°C for 30s	yes	yes	yes	yes	yes	yes	yes	yes
6-10	Td Preheat	220°C for 30s	yes	yes	yes	yes	yes	yes	yes	yes
11-15	Td Preheat	240°C for 30s	yes	yes	yes	yes	yes	yes	yes	yes
16-20	Td Preheat	260°C for 30s	yes	yes	yes	yes	yes	yes	yes	yes
1-20	Test Measurement	OSL 60s at 125°C	yes	yes	yes	yes	yes	yes	yes	yes

Table 4-1: Quartz Single Aliquot Regenerative (SAR) Sequence (Discs 1 -16)

4.3. Results

4.3.1. Dose rates

HRGS results are shown in Table 4-1, both as activity concentrations (i.e. disintegrations per second per kilogram) and as equivalent parent element concentrations (in % and ppm), based in the case of U and Th on combining nuclide specific data assuming decay series equilibrium. K, U and Th concentrations ranged between 1.7 and 2.1 %, 1.9 and 3.2 ppm and 4.7 to 8.7 ppm, respectively. Infinite matrix alpha, beta and gamma dose rates from HRGS are listed for all samples in Table 4-2, together with infinite matrix beta dose rates from TSBC. Gamma dose rates, as measured on dry samples in the laboratory, ranged between 0.89 ± 0.02 to 1.31 ± 0.02 mGy a⁻¹, with a mean value of 1.06 ± 0.15 mGy a⁻¹. Beta dose rates measured by HRGS ranged between 1.90 ± 0.04 to 2.46 ± 0.04 mGy a⁻¹, with a mean value of 2.13 ± 0.19 mGy a⁻¹. TSBC beta dose rate estimates ranged between 1.92 ± 0.07 to 2.40 ± 0.08 mGy a⁻¹, with a mean value of 2.14 ± 0.20 mGy a⁻¹. It is noted that there is a good agreement between the beta dose rates determined by HRGS and TSBC (the mean value obtained for the HRGS:TSBC ratio was 1.00 ± 0.20).

SUTL no.	Activity Concentration (Bq kg ⁻¹) ^a			Equivalent Concentration ^b		
	⁴⁰ K	U	Th	K (%)	U (ppm)	Th (ppm)
2580	533 ± 12	36 ± 2	29 ± 1	1.72 ± 0.04	2.92 ± 0.13	7.19 ± 0.17
2581	627 ± 13	28 ± 1	31 ± 1	2.03 ± 0.04	2.26 ± 0.11	7.56 ± 0.16
2583	583 ± 12	29 ± 1	23 ± 1	1.88 ± 0.04	2.32 ± 0.11	5.59 ± 0.15
2584	565 ± 12	23 ± 1	19 ± 1	1.83 ± 0.04	1.86 ± 0.09	4.79 ± 0.14
2585	615 ± 13	25 ± 1	21 ± 1	1.99 ± 0.04	2.05 ± 0.10	5.09 ± 0.15
2580b	652 ± 13	39 ± 2	35 ± 1	2.11 ± 0.04	3.16 ± 0.14	8.57 ± 0.17
2581b	658 ± 13	35 ± 2	35 ± 1	2.13 ± 0.04	2.87 ± 0.13	8.74 ± 0.18
2583b	572 ± 12	32 ± 1	21 ± 1	1.85 ± 0.04	2.56 ± 0.12	5.14 ± 0.15
2584b	556 ± 12	23 ± 1	19 ± 1	1.80 ± 0.04	1.89 ± 0.09	4.67 ± 0.14
2585b	580 ± 12	27 ± 1	23 ± 1	1.88 ± 0.04	2.15 ± 0.10	5.78 ± 0.14

Table 4-2: Activity and equivalent concentrations of K, U and Th determined by HRGS

^aShap granite reference, working values determined by David Sanderson in 1986, based on HRGS relative to CANMET and NBL standards.

^bActivity and equivalent concentrations for U, Th and K determined by HRGS (Conversion factors based on NEA (2000) decay constants): 40K: 309.3 Bq kg⁻¹ %K⁻¹, 238U: 12.35 Bq kg⁻¹ ppmU⁻¹, 232Th: 4.057 Bq kg⁻¹ ppm Th⁻¹.

It is notable that the equivalent concentrations obtained from the sediment samples obtained from profiles USU13-1 and -2 are within the range of values obtained for the samples collected in 2012; which yielded mean K, U and Th concentrations of between 1.8 and 2.5 %, 1.0 and 5.4 ppm and 3.0 to 10.9 ppm (see Kinnaird et al., 2012).

SUTL no.	HRGS, dry (mGy a ⁻¹) ^a			TSBC, dry (mGy a ⁻¹)
	Alpha	Beta	Gamma	
2580	13.44 ± 0.38	2.06 ± 0.04	1.12 ± 0.02	2.35 ± 0.08
2581	11.87 ± 0.32	2.23 ± 0.04	1.14 ± 0.02	2.35 ± 0.08
2583	10.59 ± 0.32	2.06 ± 0.04	1.01 ± 0.02	1.92 ± 0.07
2584	8.71 ± 0.28	1.92 ± 0.04	0.90 ± 0.02	2.04 ± 0.07
2585	9.45 ± 0.29	2.10 ± 0.04	0.98 ± 0.02	2.07 ± 0.07

2580b	15.12 ± 0.40	2.46 ± 0.04	1.31 ± 0.02	2.34 ± 0.08
2581b	14.44 ± 0.38	2.44 ± 0.04	1.29 ± 0.02	2.40 ± 0.08
2583b	10.91 ± 0.34	2.06 ± 0.04	1.00 ± 0.02	1.92 ± 0.07
2584b	8.71 ± 0.27	1.90 ± 0.04	0.89 ± 0.02	1.96 ± 0.07
2585b	10.25 ± 0.3	2.04 ± 0.04	1.00 ± 0.02	2.03 ± 0.07

Table 4-3: Infinite matrix dose rates determined by HRGS and TSBC.

^abased on dose rate conversion factors in Aikten (1983) and Sanderson (1987)

The water content measurements with assumed values for the average water content during burial are given in Table 4-3. The table also lists the gamma dose rate from the HRGS after application of a water content correction. Effective dose rates to the HF etched 200 µm quartz grains are given for the gamma dose rate and beta dose rate (the mean of the TSBC and HRGS data, accounting for water content and grain size).

SUTL No.	Water Content (%)			Effective Dose Rate (mGy a ⁻¹)		
	Fractional	Saturated	Assumed	Beta ^a	Gamma	Total ^b
2580	9.9	27.8	19 ± 9	1.68 ± 0.15	1.00 ± 0.06	2.86 ± 0.16
2581	11.9	24.8	18 ± 6	1.74 ± 0.13	1.01 ± 0.05	2.93 ± 0.14
2583	14.1	31.0	23 ± 8	1.44 ± 0.13	0.82 ± 0.05	2.45 ± 0.14
2584	8.3	27.2	18 ± 9	1.45 ± 0.13	0.75 ± 0.05	2.38 ± 0.14
2585	5.2	24.1	15 ± 9	1.58 ± 0.14	0.85 ± 0.06	2.60 ± 0.16

Table 4-4: Water contents, and effective beta and gamma dose rates following water correction.

^aEffective beta dose rate combining water content corrections with inverse grain size attenuation factors obtained by weighting the 200 µm attenuation factors of Mejdahl (1979) for K, U, and Th by the relative beta dose contributions for each source determined by Gamma Spectrometry.

4.3.2. Single aliquot equivalent dose determinations

For equivalent dose determination, data from single aliquot regenerative dose measurements were analysed using the Risø TL/OSL Viewer programme to export integrated summary files that were analysed in MS Excel and SigmaPlot. Composite dose response curves were constructed from selected discs and for each of the four preheating groups from each sample, and used to estimate equivalent dose values for each individual disc and their combined sets. Dose response curves for each of the four preheating temperature groups and the combined data were determined using a fit to exponential function (Appendix B). The equivalent dose was then determined for each aliquot using the corresponding exponential fit parameters.

The distribution in equivalent dose values was examined using radial plotting methods (Appendix C). All samples revealed some heterogeneity in their equivalent dose distributions. Single aliquots were rejected from further analysis based on the test dose sensitivity check, SAR criteria checks, the robust mean, feldspar contamination and radial plots. Table 4-4 summarises the quality evaluation checks on the SAR data (once filtered); the mean sensitivity of each aliquot and sensitivity change, the recycling ratio and zero dose response.

SUTL No.	Mass (mg)	Sensitivity (counts/Gy)	Sensitivity change (%)	Recycling Ratio	Zero Dose (Gy)	IRSL response (%)
2580	2.50	2718 ± 1041	17.23 ± 6.38	1.03 ± 0.02	0.39 ± 0.06	10.08 ± 1.77
2581	2.40	2909 ± 398	3.38 ± 0.63	1.01 ± 0.02	-0.07 ± 0.30	5.52 ± 0.86
2583	2.33	752 ± 104	2.96 ± 0.66	0.98 ± 0.02	0.23 ± 0.05	3.65 ± 0.95
2584	2.13	3541 ± 594	-6.24 ± 2.56	0.98 ± 0.01	0.18 ± 0.05	24.24 ± 3.11
2585	2.16	1967 ± 506	2.22 ± 0.91	1.02 ± 0.02	0.48 ± 0.19	10.65 ± 3.17

Table 4-5: SAR quality parameters. Standard errors given.

4.3.3. Age determinations

The total dose rate is determined from the sum of the equivalent beta and gamma dose rates, and the cosmic dose rate. Age estimates are determined by dividing the equivalent stored dose by the dose rate. Uncertainty on the age estimates is given by combination of the uncertainty on the dose rates and stored doses, with an additional 5% external error. Table 4-6 lists the total dose rate, stored dose and corresponding age of the sample.

SUTL No.	Section	Distance from datum / cm	Dose Rate (mGy a ⁻¹)	Comments on Equivalent Dose Distribution/age distributions	Stored Dose (Gy)	Years BP	Calendar years
2580	USU13-1	45*	2.86 ± 0.16	Broad equivalent dose distribution; however, all aliquots within 2σ of the linear and weighted means	1.25 ± 0.11	0.44 ± 0.05	1570 ± 50
2581		110*	2.93 ± 0.14	Broad equivalent dose distribution; however, 13 aliquots within 2σ of the weighted mean	1.69 ± 0.07	0.58 ± 0.04	1430 ± 40
2583	USU13-2	195 [†]	2.45 ± 0.14	Complex equivalent dose populations; 11 aliquots within 2σ of the weighted mean - 0.77 ± 0.05 Gy; 5 aliquots tail towards a higher stored dose estimate, mean 1.6 ± 0.3 Gy	0.77 ± 0.05	0.31 ± 0.03	1700 ± 30
2584		95 [†]	2.38 ± 0.14	Complex equivalent dose populations; 9 aliquots within 2σ of the weighted mean - 1.54 ± 0.07 Gy; 6 aliquots tail towards a higher stored dose estimate, mean 2.6 ± 0.2 Gy; 1 low outlier at 0.9 Gy; 1 high outlier in excess of 18 Gy	1.54 ± 0.07	0.65 ± 0.05	1360 ± 50
2585		45 [†]	2.60 ± 0.16	Complex equivalent dose populations; 11 aliquots within 2σ of the weighted mean - 0.68 ± 0.05 Gy; 6 aliquots tail towards a higher stored dose estimate, mean 1.4 ± 0.1 Gy; 1 high outlier in excess of 6 Gy	0.68 ± 0.05	0.26 ± 0.02	1750 ± 30

Table 4-6: OSL age determinations for samples SUTL2580-81 and 2583-84

*depth in section; [†]height in section

5. Discussions and conclusions

The combination of luminescence profiling, and quantitative quartz OSL SAR dating, has permitted the construction of a luminescence chronology, for the terrace deposits of the Usumacinta River. The initial field profiling suggested that the stratigraphy within each profile was complex, with cyclic variations in net signal intensities, from maxima (or peaks) in signal intensities, followed by a non-linear trend to low signal intensities, possibly reflecting initial high-energy flushing, or transportation, of sediment through the system (bringing in material with high residuals), to waning, low-energy flows, in which the luminescence signals can be reset. The subsequent calibrated luminescence screening dataset, in the form of stored dose-depth and sensitivity-depth profiles, permitted the appraisal of local variations in sediment flux and rates. Full quartz OSL SAR dating were then instigated as a means of defining the chronology for the Usumacinta River, within this culturally sensitive part of the river basin, through the post-Classical Mayan period and early modern periods of Mexican history.

It is well recognised that fluvial sediments of this sort have the potential for enclosing mixed-age populations, and indeed the dose distributions obtained from three of the five samples, show some aliquots which tail to higher apparent ages; reflecting poor bleaching at the time of deposition and/or mixing of poorly bleached and unbleached material. Nevertheless, through statistical analysis, dating results were obtained for both sections that are internally consistent, and provide a chronology to interpret the changing fluvial dynamics of the Usumacinta River, and a valuable tool to observe flood events through the historical period. Two of the five samples, both from USU13-1, yielded slightly tighter equivalent dose distributions, suggesting that for these samples, the luminescence signals were better reset at deposition. The quartz OSL SAR ages obtained for USU13-1, range from AD 1430 \pm 40 (SUTL2581; at depth, 110 cm) to AD 1570 \pm 50 (SUTL2580; at 45 cm), implying that these sediments accumulated in the post-Classical Mayan period. The remaining three samples, all from section USU13-2, showed some scatter in equivalent doses, with some aliquots tailing to a higher apparent dose, and thus age. For these samples, the corresponding radial plots (see Appendix D), provide a means of assessing the different age components. For each, the aliquots forming the main 'component' or 'cluster' of equivalent doses, fall within 2σ of the weighted mean, and accordingly these estimates were used to calculate the age. Using this method, quartz OSL SAR ages of AD 1700 \pm 30, AD 1360 \pm 50 and AD 1750 \pm 30 were obtained for the strata at 195 cm, 95 cm and 45 cm height in the succession. Intriguing, the sub-population of aliquots, which tail to older apparent ages, from samples SUTL2583 and 2585, are similar to the weighted mean of all aliquots from SUTL2584; suggesting that all strata sampled in USU13-2, may have been sourced from a 15th century or older sediment accumulation upstream. Interestingly, a 15th century date for the upstream accumulation, would place it within the same period of deposition as the strata dated in section USU13-1. Furthermore, the deposition of a > 2m thick accumulation of sediment within a few decades testifies to the magnitude of the severe, depositional event.

Given the cyclicity to the depositional sequence, perhaps it is the statistical combinations of the individual quartz OSL SAR ages, which give the best representation of the true accumulation age for each sequence: the fluvial sequence in

USU13-1 presumably accumulated from the late 15th century, whereas the sequence in USU13-2 accumulated in the 18th century.

6. References

- Aitken, M.J., 1983, Dose rate data in SI units: PACT, v. 9, p. 69–76.
- Bøtter-Jensen, L., Bulur, E., Duller, G.A.T., and Murray, A.S., 2000, Advances in luminescence instrument systems: Radiation Measurements, v. 32, p. 523-528.
- Mejdahl, V., 1979, Thermoluminescence dating: Beta-dose attenuation in quartz grains Archaeometry, v. 21, p. 61-72.
- Murray, A.S., and Wintle, A.G., 2000, Luminescence dating of quartz using an improved single-aliquot regenerative-dose protocol: Radiation Measurements, v. 32, p. 57-73.
- NEA, 2000, The JEF-2.2 Nuclear Data Library: Nuclear Energy Agency, Organisation for economic Co-operation and Development. JEFF Report, v. 17.
- Prescott, J.R., and Hutton, J.T., 1994, Cosmic ray contributions to dose rates for luminescence and ESR dating: Large depths and long-term time variations: Radiation Measurements, v. 23, p. 497-500.
- Sanderson, D.C.W., 1987, Thermoluminescence dating of vitrified Scottish Forts: Paisley, Paisley college.
- , 1988, Thick source beta counting (TSBC): A rapid method for measuring beta dose-rates: International Journal of Radiation Applications and Instrumentation. Part D. Nuclear Tracks and Radiation Measurements, v. 14, p. 203-207.
- Sanderson, D.C.W., and Murphy, S., 2010, Using simple portable OSL measurements and laboratory characterisation to help understand complex and heterogeneous sediment sequences for luminescence dating: Quaternary Geochronology, v. 5, p. 299-305.

Appendix A: Laboratory Profiling Results

A.1 SUTL2582/SUTL2586 Quartz

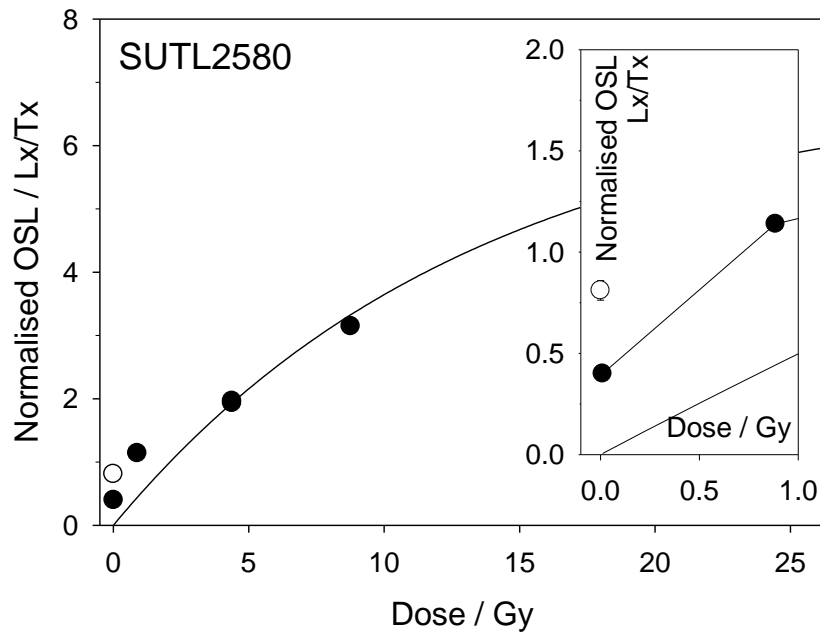
Depth /cm	SUTL no.	OSL at 125°C				TL to 500°C			
		Stored dose /Gy		Sensitivity / counts per Gy		Stored dose /Gy		Sensitivity / counts per Gy	
		Aliquot 1	Aliquot 2	Aliquot 1	Aliquot 2	Aliquot 1	Aliquot 2	Aliquot 1	Aliquot 2
Section USU13-1, Usumacinta River									
20	2582A	1.74 ± 0.04	1.26 ± 0.07	3109 ± 28	1258 ± 20	34.1 ± 7.6	257.5 ± 28.6	195 ± 7	107 ± 5
45	2580	1.80 ± 0.07	1.36 ± 0.06	2473 ± 26	2221 ± 25	75.0 ± 3.6	138.6 ± 7.3	658 ± 13	447 ± 10
60	2582B	0.79 ± 0.04	0.74 ± 0.03	2145 ± 25	2188 ± 25	137.7 ± 10.9	115.0 ± 9.7	203 ± 7	237 ± 8
80	2582C	0.90 ± 0.03	1.27 ± 0.05	3036 ± 28	2237 ± 26	151.1 ± 9.5	78.4 ± 4.6	401 ± 10	459 ± 11
110	2581	1.01 ± 0.07	1.32 ± 0.06	1083 ± 19	1691 ± 22	95.0 ± 6.2	89.8 ± 5.8	338 ± 9	338 ± 9
140	2582D	5.01 ± 0.34	2.91 ± 0.21	633 ± 15	708 ± 15	46.6 ± 9.0	269.5 ± 23.7	125 ± 6	151 ± 6
Section USU13-2, Usumacinta River									
195	2583	0.25 ± 0.02	0.51 ± 0.02	2944 ± 28	3845 ± 34	276.7 ± 16.5	62.9 ± 1.6	483 ± 11	2348 ± 24
170	2586A	0.28 ± 0.04	1.84 ± 0.12	1637 ± 22	1096 ± 18	165.7 ± 8.8	301.4 ± 17.0	470 ± 11	493 ± 11
150	2586B	0.96 ± 0.12	1.03 ± 0.09	666 ± 14	1198 ± 19	178.1 ± 12.9	147.5 ± 10.5	272 ± 8	349 ± 9
120	2586C	0.22 ± 0.03	0.26 ± 0.02	1596 ± 21	2544 ± 27	228.7 ± 24.7	72.0 ± 10.0	111 ± 5	147 ± 6
95	2584	1.91 ± 0.1	1.05 ± 0.07	1482 ± 20	1659 ± 22	270.8 ± 15.9	80.9 ± 3.7	416 ± 10	733 ± 13
70	2586D	25.9 ± 0.52	2.55 ± 0.16	4426 ± 34	1008 ± 17	597.9 ± 17.3	125.9 ± 11.5	1715 ± 20	229 ± 7
45	2585	0.9 ± 0.06	6.99 ± 0.29	1386 ± 20	1458 ± 20	231.4 ± 15.3	253.3 ± 14.8	365 ± 9	474 ± 11
20	2586E	0.41 ± 0.05	0.53 ± 0.05	1572 ± 21	1833 ± 23	294.4 ± 24.2	273.1 ± 19.0	269 ± 8	288 ± 8
0	2586F	1.53 ± 0.08	0.6 ± 0.05	2181 ± 29	1567 ± 21	103.3 ± 3.0	295.4 ± 24.6	1720 ± 20	174 ± 7

A.2 SUTL2582/SUTL2586 Polymineral

Depth /cm	SUTL no.	IRSL at 50°C		post-IR IRSL at 225°C		post-IR OSL at 125°C		post-IR TL to 500°C	
		stored dose /Gy	sensitivity /photon counts Gy ⁻¹	stored dose /Gy	sensitivity /photon counts Gy ⁻¹	stored dose /Gy	sensitivity /photon counts Gy ⁻¹	stored dose /Gy	sensitivity /photon counts Gy ⁻¹
Section USU13-1, Usumacinta River									
20	2582/A	47.2 ± 13.4	33.2 ± 17.6	939.7 ± 692.1	13.0 ± 4.7	40.1 ± 25.1	66.8 ± 16.2	2196.1 ± 839.4	37.6 ± 14.5
60	2582/B	82.1 ± 26.0	17.0 ± 3.9	266.2 ± 106.9	12.4 ± 4.2	13.9 ± 0.1	118.8 ± 51.5	729.1 ± 65.1	79.1 ± 7.2
80	2582/C	52.7 ± 10.3	31.0 ± 3.0	249.6 ± 17.7	14.4 ± 0.1	46.3 ± 36.9	134.4 ± 5.2	1347.5 ± 170.2	40.7 ± 3.3
140	2582/D	111.2 ± 21.3	35.6 ± 16.5	332.9 ± 153.5	18.6 ± 9.3	10.1 ± 1.1	262.0 ± 48.5	1082.6 ± 127.1	55.3 ± 16.3
Section USU13-2, Usumacinta River									
170	2586/A	36.1 ± 9	84.8 ± 56.3	654.1 ± 25.5	27.9 ± 11.5	15.8 ± 4.3	106.2 ± 3.9	1441 ± 109.7	77.8 ± 44.4
150	2586/B	157.4 ± 39.5	85.8 ± 12.3	767.3 ± 189.1	69.1 ± 33.4	30.9 ± 2.2	83.2 ± 23.3	3330.3 ± 992.1	69 ± 4.2
120	2586/C	77.3 ± 8.6	20.1 ± 0.7	827.4 ± 72.7	13.9 ± 2.7	33.8 ± 5.6	76 ± 2.6	3252.7 ± 412.5	35 ± 0.7
70	2586/D	80.8 ± 4.4	29.4 ± 6.3	885.9 ± 110.6	24.9 ± 0.6	11 ± 0.6	109.6 ± 6.8	2583.2 ± 356.1	41.6 ± 5
20	2586/E	122.7 ± 10.6	27.8 ± 12.7	638.1 ± 84.3	31.8 ± 8.1	20.7 ± 1	70.3 ± 9.1	4090.7 ± 2115	39 ± 9.8
0	2586/F	67.3 ± 38.3	104 ± 61.2	816 ± 354.5	40.4 ± 13	23.3 ± 14.9	137.8 ± 32.4	3076.6 ± 2296	109.3 ± 65.1

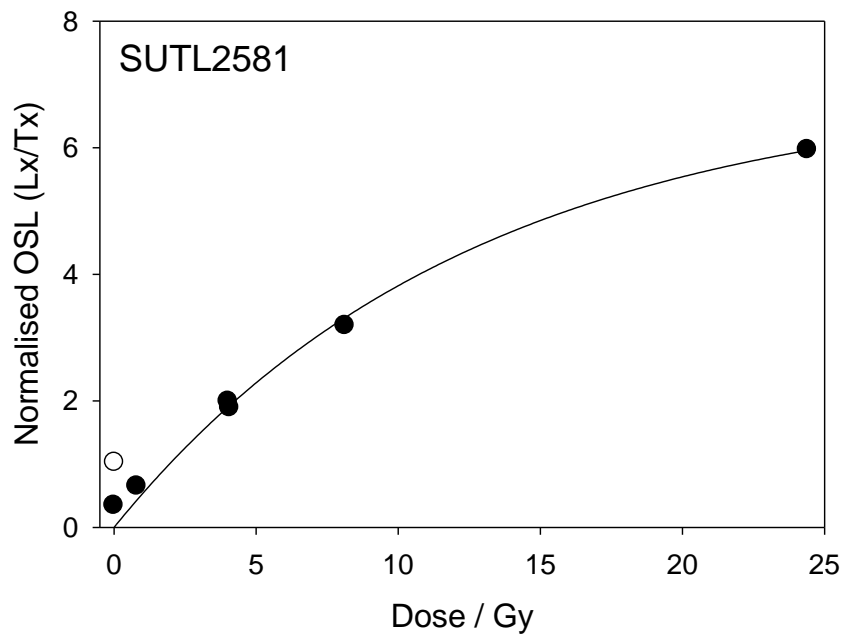
Appendix B: Dose Response Curves

B.1 SUTL2580



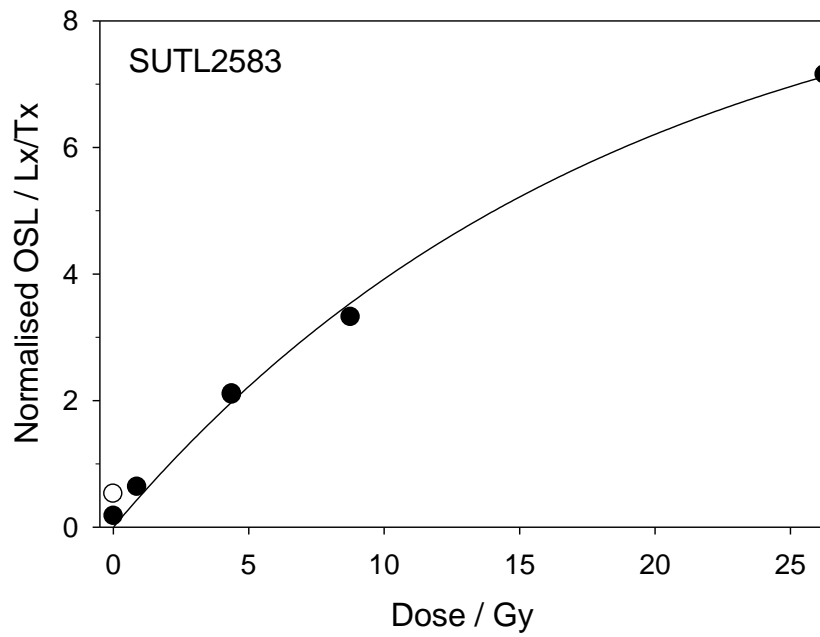
Composite dose response curve for sample SUTL2580
Lx = 0, 1, 5, 10, 30 and 5Gy;
Tx = 2 Gy

B.2 SUTL2581



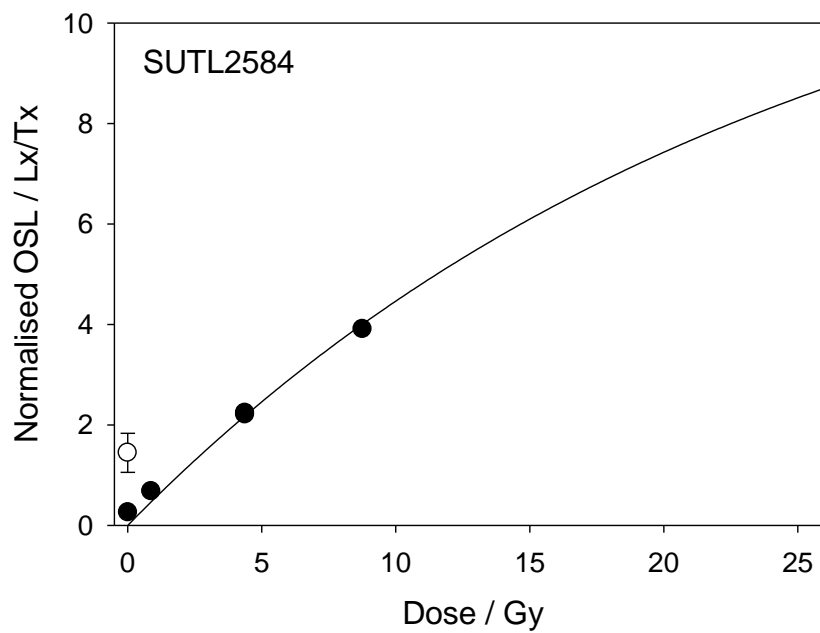
Composite dose response curve for sample SUTL2581
Lx = 0, 1, 5, 10, 30 and 5 Gy;
Tx = 2 Gy

B.3 SUTL2583



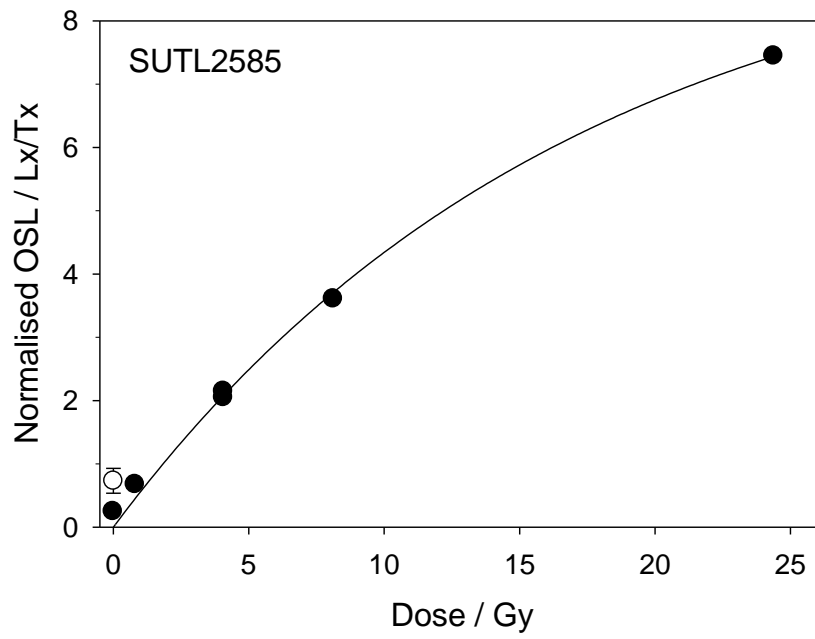
Composite dose response curve for sample SUTL2583
Lx = 0, 1, 5, 10, 30 and 5Gy;
Tx = 2 Gy

B.4 SUTL2584



Composite dose response curve for sample SUTL2584
Lx = 0, 1, 5, 10, 30 and 5 Gy;
Tx = 2 Gy

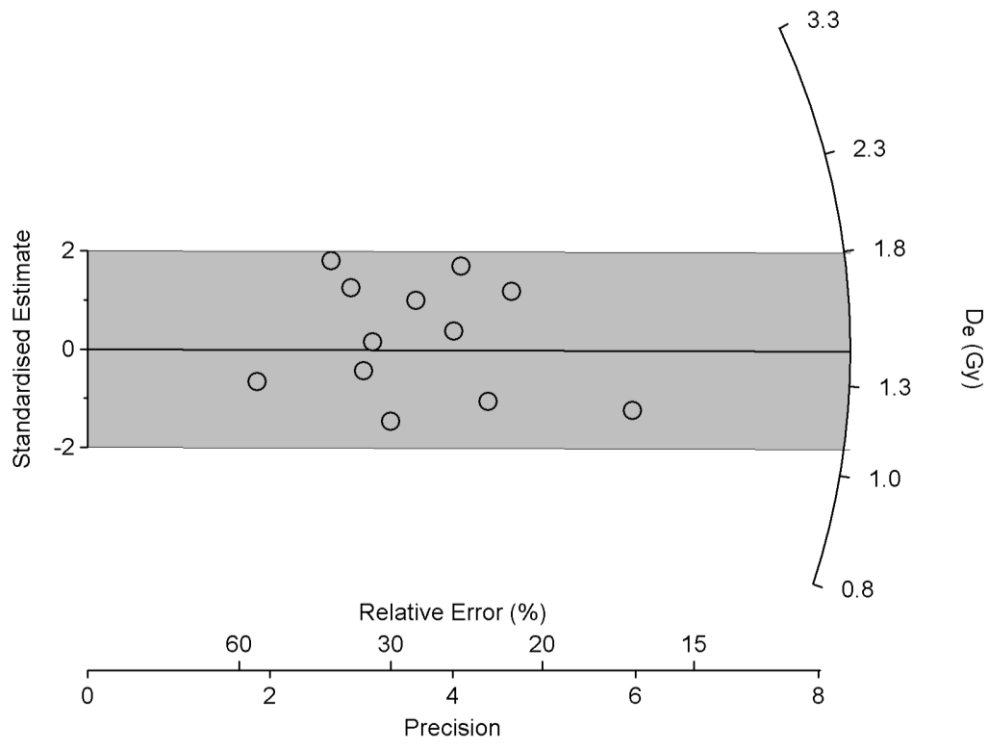
B.5 SUTL2585



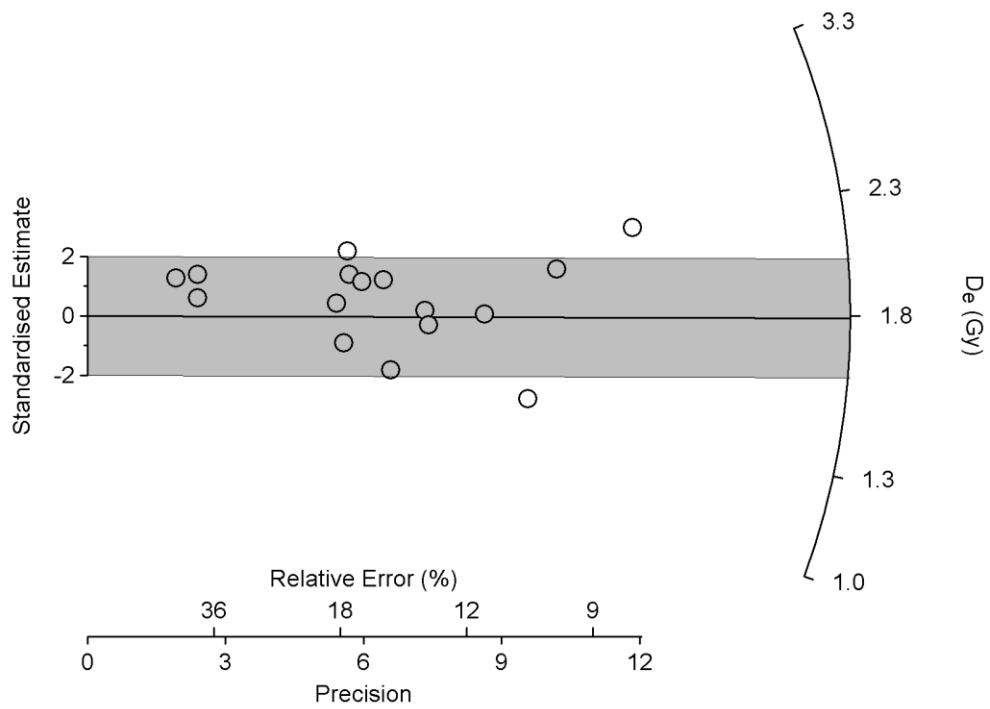
Composite dose response curve for sample SUTL2585
Lx = 0, 1, 5, 10, 30 and 5 Gy;
Tx = 2 Gy

Appendix D: Radial plots

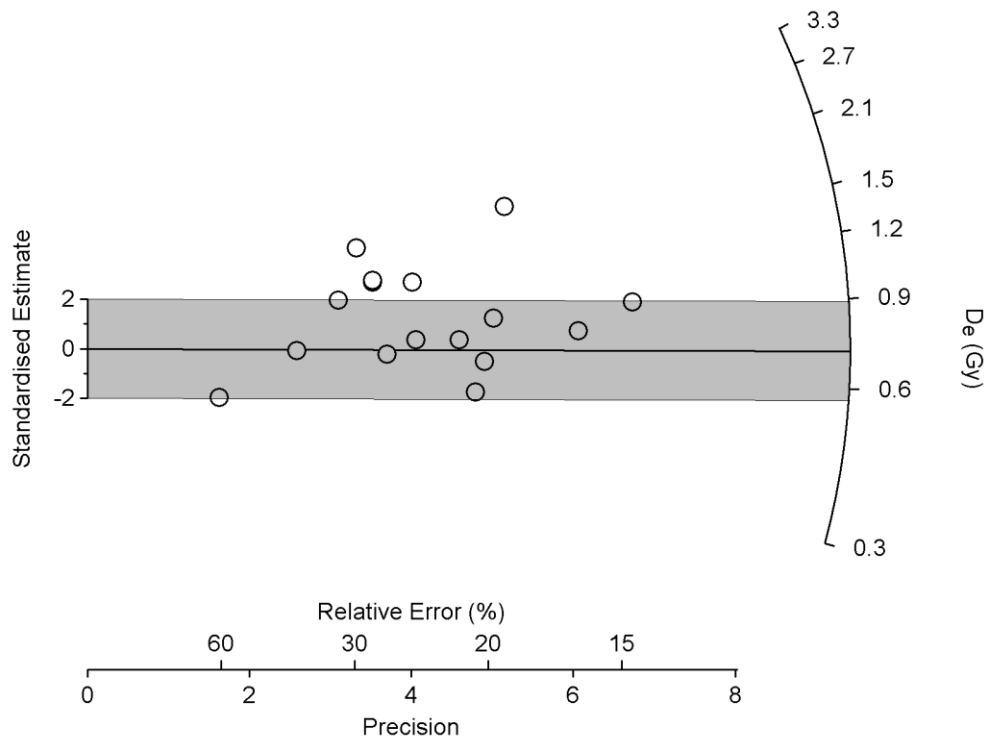
D.1 Radial plot for SUTL2580



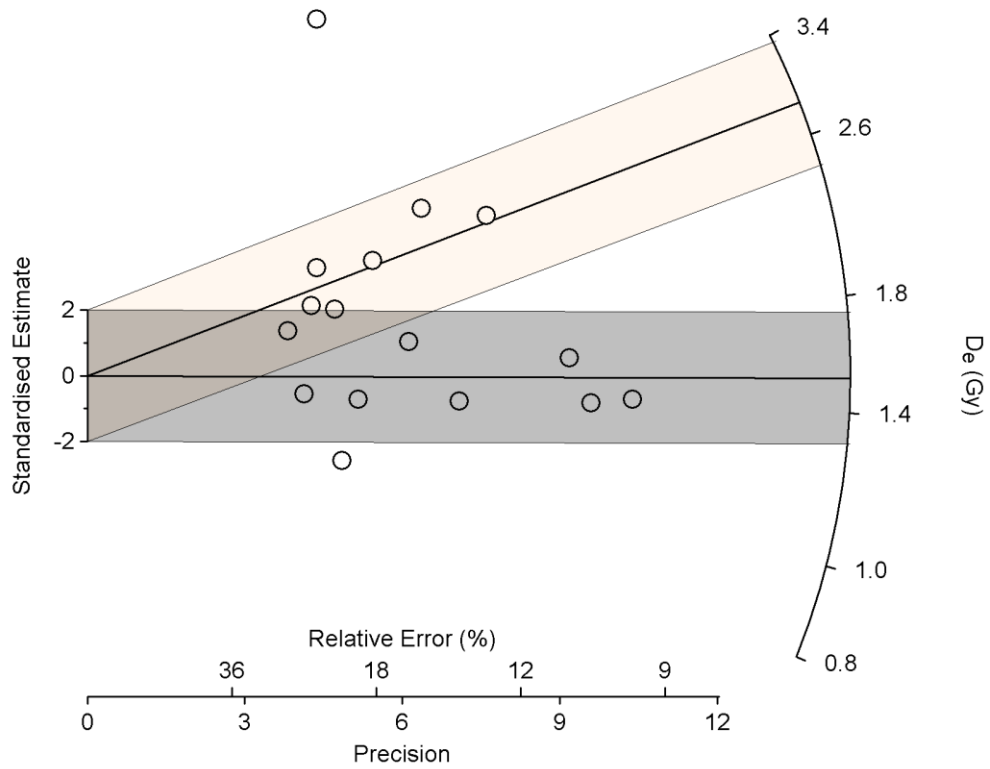
D.2 Radial plot for SUTL2581



D.3 Radial plot for SUTL2583



D.4 Radial plot for SUTL2584



D.5 Radial plot for SUTL2585

